

Development and Use of Clickable Activity Based Protein Profiling Agents for Protein Arginine Deiminase 4

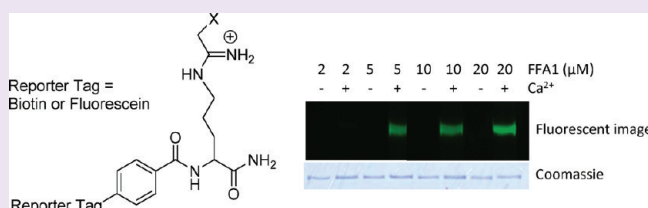
Jessica L. Slack,^{†,‡} Corey P. Causey,[†] Yuan Luo,[†] and Paul R. Thompson^{†,‡,*}

[†]The Department of Chemistry and Biochemistry, University of South Carolina, 631 Sumter St., Columbia, South Carolina 29208, United States

[‡]Department of Chemistry, The Scripps Research Institute, 120 Scripps Way, Jupiter, Florida 33458, United States

S Supporting Information

ABSTRACT: The protein arginine deiminases (PADs), which catalyze the hydrolysis of peptidyl-arginine to form peptidyl-citrulline, are potential targets for the development of a rheumatoid arthritis (RA) therapeutic, as well as other human diseases including colitis and cancer. Additionally, these enzymes, and in particular PAD4, appear to play important roles in a variety of cell signaling pathways including apoptosis, differentiation, and transcriptional regulation. To better understand the factors that regulate *in vivo* PAD4 activity, we set out to design and synthesize a series of activity-based protein profiling (ABPP) reagents that target this enzyme. Herein we describe the design, synthesis, and evaluation of six ABPPs including (i) FITC-conjugated F-amidine (FFA1 and 2) and Cl-amidine (FCA1 and 2), and (ii) biotin-conjugated F-amidine (BFA) and Cl-amidine (BCA). We further demonstrate the utility of these probes for labeling PAD4 in cells, as well as for isolating PAD4 and PAD4 binding proteins. These probes will undoubtedly prove to be powerful tools that can be used to dissect the factors controlling the dynamics of PAD4 expression, activity, and function.



Protein arginine deiminases (PADs) catalyze the hydrolytic conversion of arginine residues to citrulline residues.^{1,2} Significant recent efforts have been made toward understanding the physiological roles of these protein modifying enzymes, and in particular PAD4, due to the increasing evidence linking dysregulated PAD activity to the increased incidence and severity of rheumatoid arthritis (RA) and other diseases, including colitis and cancer.^{1,3,4} To date, PAD4 has been shown to play important roles in numerous cell signaling pathways, including differentiation and apoptosis.⁵ The best characterized *in vivo* role of PAD4, albeit still partially undefined, is that of a transcriptional regulator.^{6–11} For example, multiple arginine residues in the N-terminal tails of histones H2A, H3, and H4 are deiminated by PAD4, and the deimination of these residues has recently been shown to correlate with the down regulation of numerous genes that are controlled by the estrogen receptor, thyroid receptor, and p53.^{6–11} Although it is evident that PAD4 plays an important role in human cell signaling, it remains unclear how this enzyme is activated within the cell. Previous studies have demonstrated that up to 5 calcium ions are required for PAD4 activity *in vitro*; calcium binding induces a conformational change that orients active site residues into positions that are competent for catalysis.^{12–14} However, the concentration of calcium required for maximal PAD4 activity *in vitro* is in the high micromolar to low millimolar range, whereas normal intracellular concentrations of calcium are in the nanomolar to low micromolar range.^{13,15–17} Therefore, gaining an understanding of how PAD4 becomes active at physiological

calcium levels is essential to understanding the *in vivo* roles of this enzyme.

To better appreciate the mechanisms that regulate *in vivo* PAD4 activity, we set out to design and synthesize a series of activity-based protein profiling (ABPP) reagents that target this enzyme. We chose to develop these reagents because (i) ABPPs have proven to be invaluable tools for identifying and characterizing a diverse number of enzyme families, *e.g.*, serine hydrolases, cysteine proteases, and kinases,^{18–20} and (ii) our ABPPs will be useful for answering a number of fundamental questions regarding PAD4 activation. For example, these probes will allow us to identify PAD4 binding proteins, as well as the post-translational modifications (PTMs) that occur to this enzyme *in vivo*, and determine whether these PTMs and binding proteins modulate PAD4 activity.

ABPPs typically contain two core elements: (i) a reactive group that modifies the active site of the protein of interest and (ii) a reporter tag, typically either a fluorophore for rapid and sensitive detection of the enzyme-ABPP-conjugate or, alternatively, a biotin tag to facilitate the isolation of probe-modified proteins in complex proteomes. The basic design of the reactive portion of our PAD4-targeted ABPPs centers on F- and Cl-amidine, two previously described mechanism-based PAD4 inactivators (Figure 1A)^{21,22}

Received: November 2, 2010

Accepted: January 25, 2011

Published: January 25, 2011

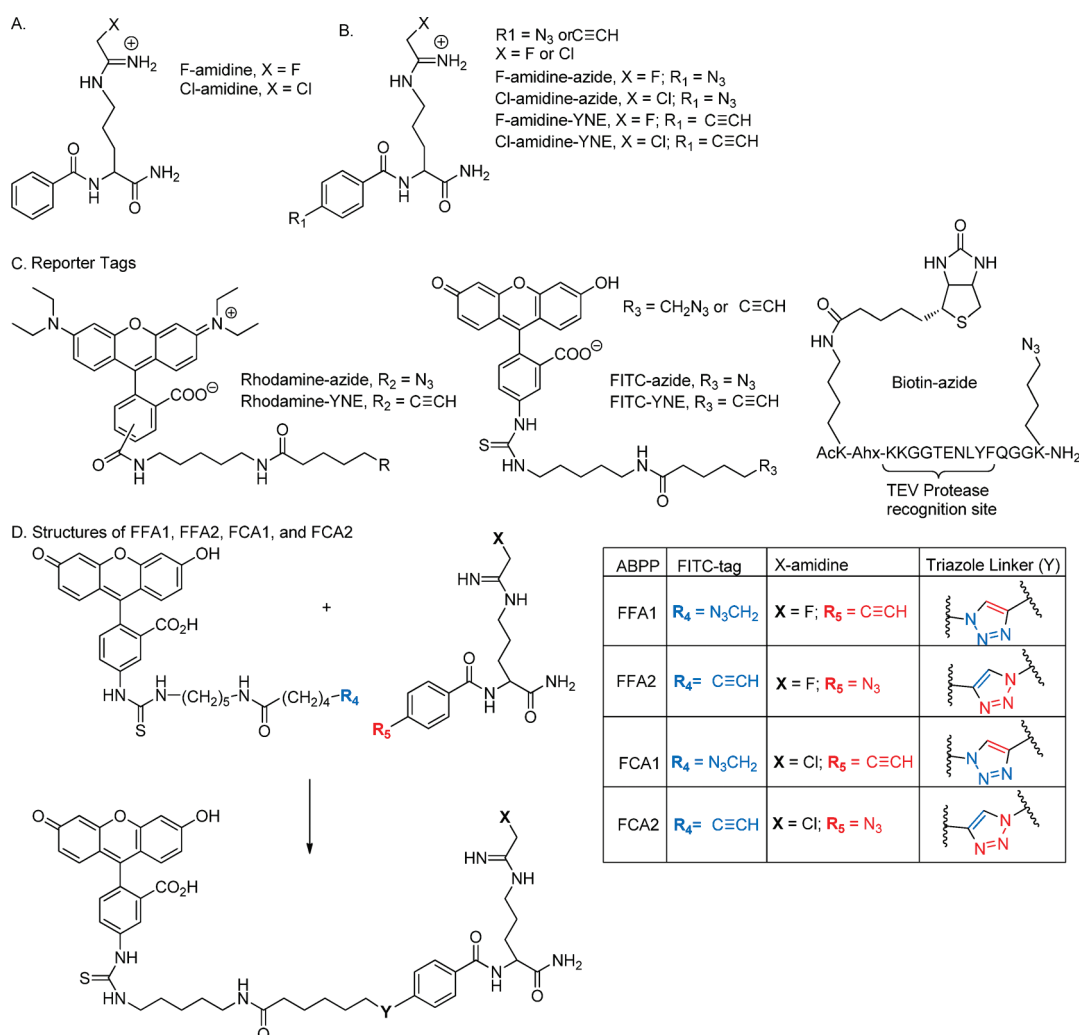


Figure 1. Structures of PAD4 targeted ABPPs. (A) Structures of F- and Cl-amidinium. (B) Structures of azide or alkyne bearing ABPPs. (C) Structures of reporter tags. (D) Structures of FFA1, FFA2, FCA1, and FCA2.

that possess a haloacetamidinium moiety,^{21–23} which covalently modifies a key catalytic residue, *i.e.*, Cys645, to effect enzyme inactivation. Alkylation of Cys645 by these compounds proceeds through one of two potential mechanisms. In the first mechanism, Cys645 directly displaces the halide through an S_N2 mechanism. Alternatively, inactivation may proceed *via* a multistep mechanism that involves an initial attack of Cys645 on the iminium carbon, followed by the protonation and stabilization of the tetrahedral intermediate, which facilitates the halide-displacement reaction.^{21,22,24} Because F- and Cl-amidinium preferentially modify calcium-bound PAD4, *i.e.*, the active form of the enzyme, these compounds lend themselves well to providing the reactive portion of our PAD4-targeted ABPPs.^{21,22}

Given that the presence of a bulky fluorophore or biotin reporter tag may limit cell permeability,^{18,19,25} we incorporated bio-orthogonal “click” chemistry compatible reactive groups into the design of these ABPPs. As previously described for other systems, including the arginine deiminases,^{19,20,26,27} the reactive portion of the ABPP contains either an alkyne or azide moiety that can react with a complementary azide/alkyne reporter tag *via* the azide–alkyne copper(I)-catalyzed cycloaddition reaction,^{28,29} yielding a stable triazole product that corresponds to the full ABPPs.²⁵ A key advantage of this approach is that the reactive

group (*e.g.*, azide- or alkyne-modified F- or Cl-amidinium) can be administered to living cells, thereby allowing for protein labeling to occur *in vivo*. The subsequent click chemistry then allows the modified proteins to be labeled with a reporter tag after cell lysis. We previously reported the functionalization of F- and Cl-amidinium with a rhodamine tag and showed that these compounds, which are denoted RFA and RCA (for rhodamine-conjugated F- and Cl-amidinium), could be used to directly label PAD4 *in vitro* or when the enzyme is present in *E. coli* cell extracts.³⁰ The one drawback of the previously described compounds is that the bulky fluorophore would likely limit/alter cell permeability. To overcome this issue, we report herein the synthesis and characterization of F- and Cl-amidinium derivatives bearing either an azide or alkyne functionality as well as six ABPPs including (i) FITC-conjugated F-amidinium (FFA1 and 2) and Cl-amidinium (FCA1 and 2) and (ii) biotin-conjugated F-amidinium (BFA) and Cl-amidinium (BCA) (Figure 1). Note that the biotin-conjugated ABPPs contain a tobacco etch virus (TEV) protease recognition sequence that facilitates the selective removal of the biotin tag after isolation of the target protein (Figure 1). Additionally, we report the optimized conditions for the post-inactivation coupling of the azide/alkyne bearing reporter tags to the corresponding alkyne/azide bearing ABPPs, and demonstrate

their utility for isolating PAD4 as well as PAD4 binding proteins. The research described herein highlights the utility of these ABPPs for profiling the dynamics of PAD4 expression, activity, and function.

RESULTS AND DISCUSSION

Synthesis. Given our previous success in developing rhodamine-conjugated halo-acetamide based ABPPs for PAD4,³⁰ we set out to synthesize fluorescein- and biotin-containing derivatives so that we might expand the number of tools available for studying this enzyme. Note that the fluorescein derivatives were synthesized because fluorescein is more effective under alkaline conditions, whereas rhodamine is most effective in acidic environments, a fact that can diminish the limits of detection when analyzing labeled proteins contained within gels. Thus, by developing ABPPs that contain either rhodamine or fluorescein, we expected to generate tools that would allow for optimal visualization of labeled proteins across the entire pH spectrum. The development of the fluorescein containing ABPPs began with the synthesis of two fluoroscein tags: one tag (FITC-YNE) contains a terminal alkyne moiety, and the other (FITC-azide) contains a terminal azide moiety. In each case, these tags can be “clicked” together with a complementary azide/alkyne-containing molecule (Figure 1). Synthesis of these two tags proceeded smoothly over 3 steps (Scheme S1A in Supporting Information). The first step of the syntheses involved the coupling of a carboxylic acid that contained either an azide or alkyne group to a mono-Boc-protected diamine. The protecting group was then removed with neat TFA to reveal a free amine that was subsequently reacted with fluorescein isothiocyanate (FITC) to yield the final products in respectable yields.

The azido derivatives of F- and Cl-amidine, which were previously reported by our group, were synthesized using a solid phase procedure.³⁰ The ethynyl derivatives were synthesized in a nearly identical manner (Scheme S1B). Although each of these four compounds can be conjugated to the complementary fluorescein tag, thus yielding a total of four different probes, the coupling efficiencies of FITC-N₃ and the ethynyl X-amidines was much better than the reaction between the alternative azide/alkyne set. Given that extended reaction times did not yield increased product formation, it is possible that the phenyl azide may be undergoing either reduction or decomposition over the course of the reaction. In light of these findings, which are supported by labeling experiments, we suggest that the azide/alkyne pairs that lead to FCA1 and FFA1 are the more useful of these ABPPs.

In addition to developing fluorescent ABPPs to probe PAD activity, we also saw the need for ABPPs that would facilitate both the isolation and enrichment of PAD4, thereby providing an analysis method that is even more sensitive than fluorescence imaging. To accomplish both of these goals, we chose to utilize a previously described biotin-containing reporter tag.³¹ This reporter tag, which was developed by Cravatt and colleagues and is denoted TEV-biotin-azide (Figure 1C), contains three elements: (i) a Lys-azide group that can react with ethynyl-modified F- and Cl-amidine *via* the copper(I)-catalyzed click reaction; (ii) a biotin moiety that allows for the enrichment of ABPP-modified proteins on streptavidin-agarose and/or the visualization of modified proteins by Western blot; and (iii) a TEV protease site that facilitates the selective removal of the biotin tag after isolation of the target protein. Given the enhanced reactivity of

Table 1. IC₅₀ Values

compound	IC ₅₀ with Ca ²⁺ (μM)	IC ₅₀ w/out Ca ²⁺ (μM)
F-amidine-azide	4.8 ± 0.5	>250
Cl-amidine-azide	5.7 ± 0.6	120 ± 15
F-amidine-YNE	20 ± 6.5	>250
Cl-amidine-YNE	5.4 ± 1.5	87 ± 9.0
RFA	24 ± 4.1	>76 ^a
RCA	7.4 ± 0.8	>50 ^a
FFA1	21 ± 1.8	>250
FCA1	36 ± 1.7	>250
BFA	14 ± 0.6	150 ± 20
BCA	14 ± 3.0	67 ± 2.3

^a Values from ref 24.

the ethynyl-X-amidines with the azide-tagged fluorophores, we focused our efforts on the azide-bearing reporter tag described above, as opposed to one containing an alkyne. The synthesis of the reporter tag proceeded smoothly according to previously established methods,³¹ and the complete ABPPs were generated by click chemistry. The resultant probes are termed biotin-conjugated F-amidine (BFA) and biotin-conjugated Cl-amidine (BCA). Also note that given the difficulties in synthesizing large quantities of FFA2 and FCA2 further analyses focused only on FFA1 and FCA1.

Inhibitory Properties of ABPPs. To evaluate the inhibitory properties of the ABPPs described herein and to determine whether or not the additional functional group (*i.e.*, the azide or alkyne) has deleterious effects on inhibitor potency, IC₅₀ values were determined using purified recombinant PAD4. Note that, like all IC₅₀'s, these values should be considered apparent measures of affinity; this is especially true because these are time-dependent irreversible inactivators. The IC₅₀ values determined in the presence of calcium are significantly lower than those obtained in the absence of this metal ion (Table 1). This observation is consistent with previous results for other PAD4 inactivators^{21,22,30} and indicates that these compounds preferentially modify the active, *i.e.*, calcium-bound, form of the enzyme. Importantly, the IC₅₀ values for these ABPPs range from 4.8 ± 0.5 to 36.0 ± 1.7 μM (Table 1) and are similar to those obtained for the parent compounds, *i.e.*, F-amidine (21.6 ± 2.1 μM) and Cl-amidine (5.9 ± 0.3 μM). Although this outcome is not unexpected, as the 4-position of the benzoyl ring of F- and Cl-amidine does not interact with any residue on PAD4 and points out toward solvent,^{12,22} these results are highly significant because they indicate the versatility of these compounds in that they can be used either before or after conjugation to the reporter tag.

Concentration Dependence of ABPPs. Having established that the ABPPs effectively inactivate PAD4, with potencies that are comparable to those of F- and Cl-amidine, the concentration dependence of labeling recombinant PAD4 with FFA1, FCA1, BFA, and BCA was evaluated. These ABPPs, over a range of several concentrations, were used to label 2.5 μg of PAD4 in both the presence and the absence of calcium. The labeled protein samples were then separated on a 12% SDS-PAGE gel, and the proteins were either visualized fluorescently or by Western blot analysis using streptavidin-conjugated horseradish peroxidase (HRP). While the ABPPs effectively labeled PAD4 at concentrations as low as 2 μM (Figure 2A), the selectivity of the chloro-containing derivatives, and in particular BCA, for the active form of the enzyme decreases at higher concentrations, as exemplified

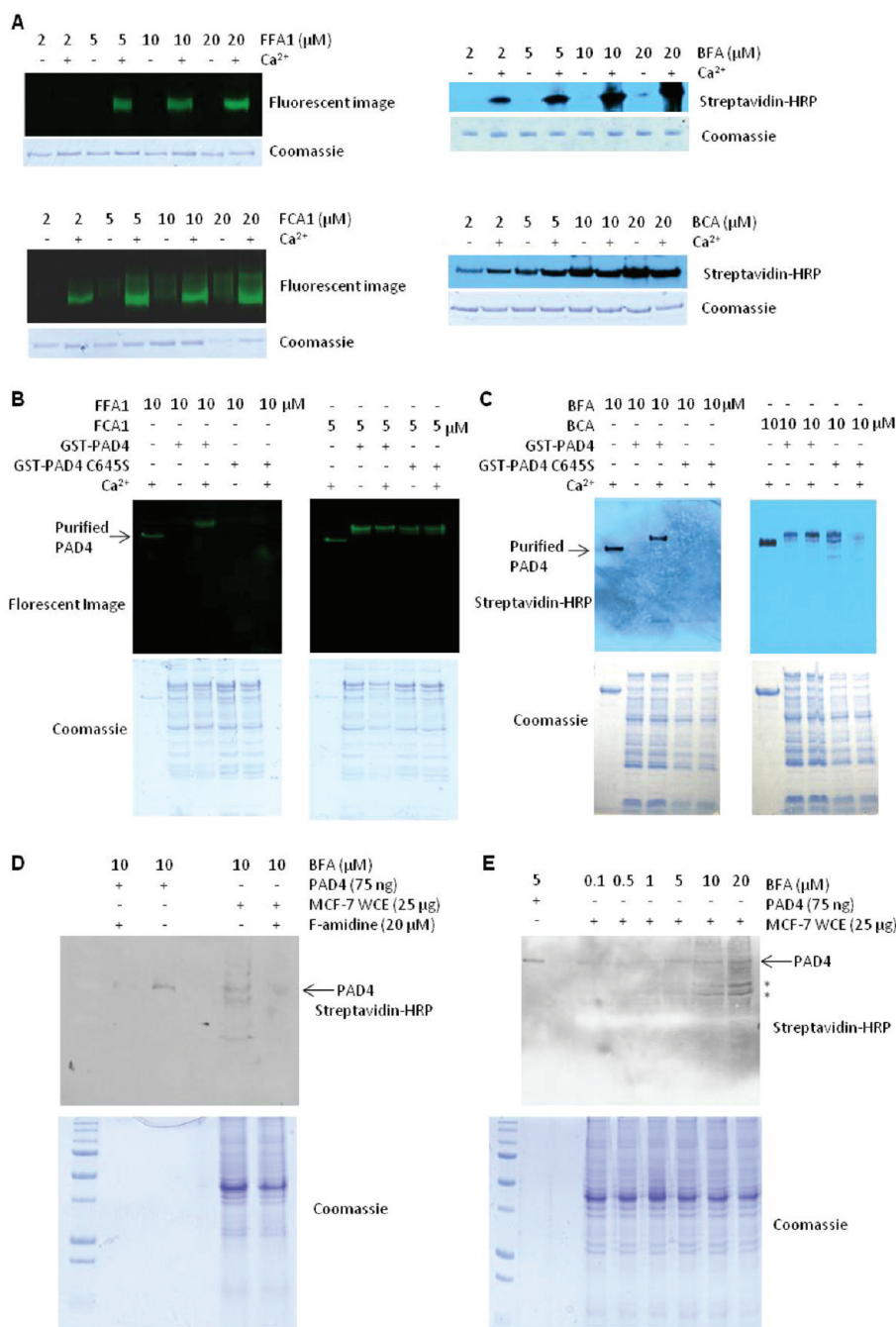


Figure 2. Characterization of PAD4-targeted ABPPs. (A) Concentration dependence: Recombinant wild type PAD4 (2.5 μg) was labeled with increasing concentrations of FFA1, FCA1, BFA, or BCA in the presence or absence of calcium. Labeled proteins were visualized either fluorescently or by Western blot using streptavidin-HRP. (B and C) Selective labeling of PAD4 in a complex protein mixture. *E. coli* extracts overexpressing GST-PAD4 or GST-PAD4C645S, a catalytically inactive mutant, were labeled with either FFA1 or FCA1 (B) or BFA and BCA (C) in either the absence or presence of calcium. Recombinant wild type PAD4 served as a positive control. Labeled proteins were visualized either fluorescently or by Western blot using streptavidin-HRP. (D and E) Labeling of endogenous PAD4 in MCF-7 WCE: (D) Recombinant PAD4 and estrogen-stimulated MCF-7 WCE were incubated with BFA in the presence of calcium for 30 min with or without F-amidine. The labeled proteins were visualized by Western blotting using streptavidin-conjugated HRP. (E) Concentration dependence of BFA labeling. MCF-7 WCE were labeled with increasing concentrations of BFA in the presence of calcium. The labeled proteins were visualized by Western blotting using streptavidin-conjugated HRP. * = likely PAD4 proteolytic fragments.

by the fact that these compounds label PAD4 in the absence of calcium. By contrast, the selectivity of FFA1 and BFA for calcium-bound PAD4 is maintained, even at the higher concentrations. These results indicate that the fluoro-bearing compounds are highly specific for the active form of the enzyme and highlight

their utility as ABPPs. Note that labeling of PAD4 with either the fluorescein- or biotin-tagged probes for 1 h yields near-quantitative labeling as only a single band is apparent in the Coomassie stained gels; the molecular weights of the fluorescein- and biotin-tagged proteins are increased by approximately 900 and 2100 Da,

respectively, and incomplete labeling would result in the appearance of two bands corresponding to unlabeled and labeled PAD4 in the Coomassie-stained gels.

Limits of Detection. To evaluate the sensitivity of the PAD4 targeted ABPPs, limit of detection experiments were conducted. These assays demonstrated that as little as 500 and 250 ng of PAD4 can be detected using FCA1 and FFA1, respectively (Figure S1). Such results are comparable to the limits of detection previously reported for the rhodamine-tagged ABPPs, *i.e.*, RFA and RCA.³⁰ Greater sensitivity is observed with the biotinylated probes; as little as 25 ng of PAD4 could be detected with BFA and BCA. The greater sensitivity is easily explained by the use of the streptavidin-conjugated HRP, which amplifies the signal, thereby lowering the detection limit.

Selective Labeling of PAD4 in Complex Protein Mixtures. The ability of FFA1, FCA1, BFA, and BCA to label PAD4 present in a complex proteome was then evaluated. To examine probe selectivity in the presence of a highly complex protein mixture, cell extracts were prepared from *E. coli* cells overexpressing either GST (glutathione *S*-transferase)-tagged PAD4 or the catalytically inactive GST-tagged C645S PAD4 mutant. Cleared cell lysates were treated with an ABPP, in either the presence or absence of calcium, and then the proteins were separated by 12% SDS-PAGE gel. Labeled proteins were visualized as described above (Figure 2B and C). Remarkably, FFA1, BFA, and to a lesser extent FCA1 and BCA, were highly selective for the calcium bound, *i.e.*, active, form of PAD4, as little to no nonspecific labeling was observed, despite the presence of a highly complex protein mixture. These results are highly significant because they indicate that these ABPPs can be used to readily label PAD4 in a complex biological environment. The fact that the catalytically inactive PAD4C645S mutant is labeled by FCA1 and BCA is likely due to the inherently greater leaving group potential of chloride. Given that chloromethylketones inactivate serine proteases *via* alkylation of the active site histidine, we considered the possibility that FCA1 and BCA label the C645S mutant *via* a similar mechanism. To address this possibility, the C645S mutant was labeled with Cl-amidine, and then aliquots were digested with GluC and Trypsin. MS analyses of the resultant peptides, which yielded 60% sequence coverage, identified peptides encompassing the unmodified active site histidine (*i.e.*, His471) and a Cl-amidine-modified serine residue (Table S1). In total, these data suggest that FCA1 and BCA label the C645S mutant on the serine residue and not the histidine.

To further characterize the utility of these probes in a more relevant setting, we examined the ability of BFA to detect endogenous PAD4 in estrogen-stimulated MCF7 whole cell extracts (WCE). Note that we focused on using BFA for these experiments because of its high sensitivity and high degree of selectivity for the active form of PAD4. Also note that estrogen-stimulated MCF-7 WCE were used because PAD4 expression is increased in response to estrogen.¹⁰ For these experiments, recombinant PAD4 and estrogen-stimulated MCF-7 WCE were incubated with BFA in the presence of calcium for 30 min with or without F-amidine. The labeled proteins were then visualized by Western blotting using streptavidin-conjugated HRP. The results of these experiments (Figure 2D) indicate that BFA cleanly labels endogenous levels (~75 ng) of PAD4 and that this labeling can be effectively blocked with F-amidine. Although two other bands are labeled in the MCF7 WCE, these fragments likely represent degradation products of PAD4 because we often observe bands of similar size in Western blots for PAD4 and because the labeling

of these proteins can be effectively competed with F-amidine. To examine the concentration dependence of labeling, MCF-7 WCE were labeled with increasing concentrations of BFA in the presence of calcium, and the labeled proteins visualized by Western blotting using streptavidin-conjugated HRP. The results of these experiments (Figure 2E) indicate that it is possible to cleanly label PAD4 at concentrations as low as 100 nM of BFA. As the concentration of BFA is increased to 20 μ M, the level of nonspecific labeling appears to increase slightly, although many of these proteins are likely PAD4 fragments, as described above.

Post-inactivation Coupling of Reporter Tags. One key advantage of the triazole linker present in these ABPPs is that it permits the use of the bio-orthogonal alkyne/azide cycloaddition reaction to couple azide or alkyne bearing versions of F- and Cl-amidine to a reporter tag bearing the complementary functionality after the lysis of cells treated with the inhibitors. This is particularly advantageous because it allows for the initial labeling step to occur in native conditions. To demonstrate the utility of this click chemistry strategy, PAD4 was reacted with F-/Cl-amidine alkyne/azide and then subsequently coupled to one of several reporter tags. These experiments were conducted with both purified recombinant PAD4 and with *E. coli* cell extracts overexpressing GST-PAD4. For these experiments, PAD4 was first reacted with either X-amidine-azide or X-amidine-YNE to afford enzyme inactivation. Subsequently, protein samples were denatured, and the cycloaddition reaction was carried out to couple the FITC reporter tags to the labeled proteins (Figure 3A and B). Each combination of inhibitor and reporter tag allowed for the successful visualization of labeled recombinant PAD4, primarily GST-PAD4, in the *E. coli* cell extracts. Importantly, the level of nonspecific labeling was low in these complex cell extracts, and no labeling was found in control experiments where the extracts were incubated with only the FITC-based reporter tags (Figure 3), thereby demonstrating these ABPPs are highly specific for PAD4. It is noteworthy that post-inactivation coupling of the reporter tags required 5 mM copper sulfate; lower amounts resulted in little to no labeled protein. This concentration of copper is higher than the levels that are traditionally used,²⁵ as well as the amount of copper required to generate the complete probes, *e.g.*, BFA. The most likely reason for this discrepancy is the presence of calcium in these reactions, which competes with copper for binding to the catalyst. It is also noteworthy that the more efficient post-inactivation coupling reactions involve the reactions of alkyne-functionalized F- and Cl-amidine with the azide-functionalized reporter tags; a comparison of the two complementary pairs can most easily be seen by comparing the labeling efficiencies in Figures 3A and B. As discussed above, the less efficient labeling with the azide-functionalized inhibitors may be due to decomposition of the aryl azide moiety. Similar results were obtained with TEV-biotin-azide (Figure 3C). These data indicate that the directionality of the cycloaddition reaction is an important consideration in the development of ABPPs of this type. Similar conclusions have been reached by Speers and Cravatt.¹⁸

Isolation of Probe-Modified Proteins. To initially evaluate the utility of these ABPPs for enriching PAD4, BFA and BCA, *i.e.*, the complete probes, were used to isolate both purified recombinant PAD4 (Figure S2A) and GST-PAD4 in present in *E. coli* extracts (Figure S2B). For these experiments, proteins were first modified with BFA and BCA. Subsequently, streptavidin agarose was added to afford the isolation of probe-modified PAD4. The results demonstrate that both BFA and BCA can be used to isolate PAD4, even from a highly complex

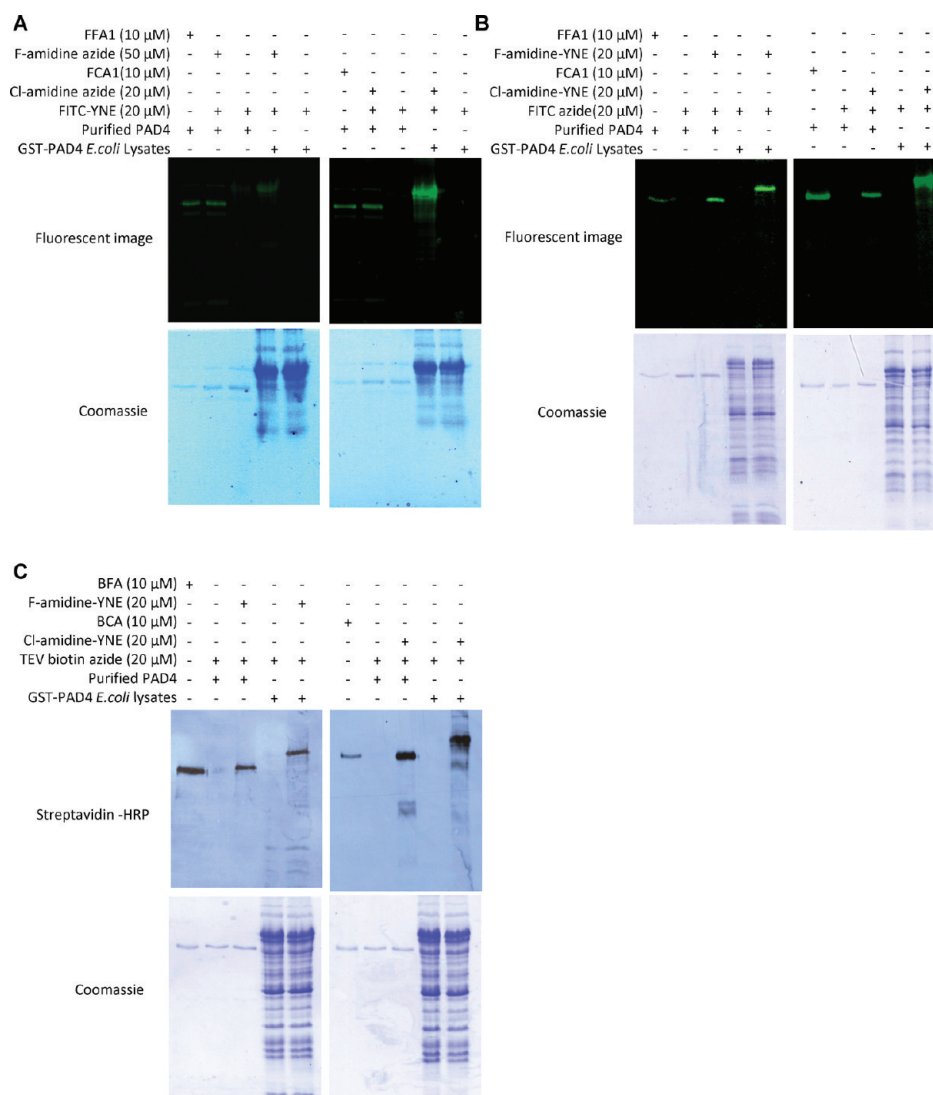


Figure 3. Post-inactivation coupling of ABPPs. Purified recombinant PAD4 or *E. coli* extracts overexpressing GST-PAD4 were reacted with either F-/Cl-amidine azide (A) or F-/Cl-amidine-YNE (B, C) and subsequently coupled to the corresponding FITC-modified tag or TEV-biotin-azide. Labeling with FFA1, FCA1, BFA, and BCA served as positive controls.

protein mixture, with negligible amounts of nonspecifically modified proteins.

To demonstrate that PAD4 can be isolated using our post-inactivation coupling procedure, pure PAD4, or GST-PAD4 present in *E. coli* cell extracts, was first reacted with F-amidine-YNE or Cl-amidine-YNE, at which point the TEV-biotin-azide reporter tag was coupled to the probe-modified proteins using the conditions established above; streptavidin-agarose was then used to isolate probe-modified proteins. As is apparent in Figure 4, post-inactivation coupling of the TEV-biotin-azide reporter tag facilitated the enrichment of both pure PAD4 (Figure 4A) and PAD4 present in a complex proteome with an efficiency similar to that obtained when using the complete ABPPs (*i.e.*, BFA and BCA; Figure 4B *versus* Figure S2). When this approach was used to isolate PAD4 from *E. coli* cell extracts, we observed an increase in the level of background proteins, which is most likely caused by protein precipitation upon addition of the copper sulfate used to catalyze the cycloaddition reaction. Although we had included the TEV protease cleavage site in our design and synthesis of the TEV-biotin-azide reporter tag, in our hands, we found that harsh

denaturing conditions, rather than use of the TEV protease cleavage site, was the most efficient method of releasing the probe-modified proteins from streptavidin-agarose (Figure S3); cleavage of the TEV site tended to be inefficient as large amounts of the protease and long incubation times were required. Although the TEV cleavage reaction occurred in low yield, the one benefit of this approach is that it appears to decrease the amount of nonspecifically bound protein released from the streptavidin-agarose. Therefore, both methods can be used to release PAD4. However, the specific method chosen should be guided by the need for yield *versus* purity, which would be dictated by subsequent methods of analysis, *e.g.*, Western blotting *versus* MS experiments.

Post-inactivation Coupling in Live MCF-7 Cells. To further illustrate the utility of these ABPPs, we set out to evaluate their utility *in cellulo*. For these experiments, MCF-7 cells, a breast adenocarcinoma cell line, were chosen because PAD4 is known to be expressed at low levels in this cell line and its expression can be enhanced by the addition of estrogen.¹⁰ PAD4 isolation experiments were conducted on both PAD4-transfected and nontransfected cells. In each case, the cells were incubated with

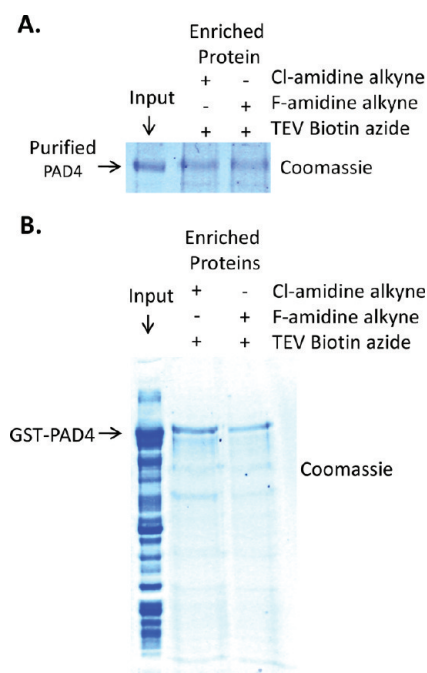


Figure 4. Enrichment of probe-modified proteins after post-inactivation coupling to TEV-biotin-azide. (A) Purified recombinant PAD4 was labeled with F- or Cl-amidinium-YNE and subsequently coupled to TEV-biotin-azide *via* click chemistry. Labeled proteins were enriched on streptavidin agarose and separated on a SDS-PAGE gel. (B) *E. coli* extracts overexpressing GST-PAD4 were labeled with either F- or Cl-amidinium-YNE. The labeled proteins were coupled to TEV-biotin-azide, enriched on streptavidin agarose, and separated on a SDS-PAGE gel.

either F- or Cl-amidinium-YNE in both the absence and presence of estrogen. Note that the alkyne versions, which are bioavailable (Figure S4), were used because we had previously shown that they can be coupled to the reporter tags with higher efficiency. After incubating the cells with inhibitors (100 μ M) for 60 min, the cells were lysed, the TEV-biotin-azide reporter tag was added, and the click reaction was initiated and allowed to proceed for 60 min. Streptavidin-agarose was then added to afford the isolation of PAD4. The results of these experiments demonstrate that these ABPPs can be used to isolate PAD4 from both transfected and nontransfected cells (Figure 5). However, we note that estrogen stimulation enhanced the levels of PAD4 isolated from nontransfected cells (compare Figure 5C *versus* D). This observation is in line with the fact that PAD4 is expressed at low levels in MCF7 cells and that its expression can be induced by the addition of estrogen, *i.e.*, the higher amounts isolated are due to the increased expression of PAD4.¹⁰ Also significant is the fact that the estrogen did not increase the amount of PAD4 isolated from the PAD4-transfected cells. Given that the fluoro-containing versions of these ABPPs are highly selective for the active enzyme, these results suggest that PAD4 is constitutively active in this cell line. It is also noteworthy that in comparison to the labeling of cell extracts with, for example, BCA, the post-inactivation coupling method afforded much cleaner results, as significantly fewer labeled proteins were apparent; the smaller labeled fragments likely correspond to proteolyzed PAD4 (Figure 6). These experiments quite conveniently demonstrate the utility of these compounds for isolating the active form of PAD4 from live cells.

Selectivity of ABPPs for Activated PAD4. To further demonstrate the utility of these probes and highlight the fact that the expression level and activity of PAD4 are independent of each other, we examined the ability of F-amidinium-YNE to label PAD4 in HL60 cells, where PAD4 is modestly active,^{7,32} and HL60 granulocytes, where PAD4 is known to be highly active.⁷ For these experiments, HL60 cells and HL60 granulocytes were first treated with F-amidinium-YNE, and then cell extracts, prepared from these cells, were coupled to TEV-biotin-azide. The probe-modified proteins were then separated by SDS-PAGE and subjected to Western blot analysis using either streptavidin-HRP or an anti-PAD4 antibody. The results of these experiments (Figure 5E) indicate that even though similar amounts of PAD4 were detected in both cell lines, labeling of PAD4 is detected only in the HL60 granulocytes. Interestingly, the labeled band is \sim 5–10 kDa smaller than full length PAD4, suggesting that, in these cells, the active form of PAD4 is a proteolytically processed form of the enzyme.

Identification of PAD4 Binding Proteins. Theoretically, the PAD4-targeted ABPPs described herein can be used to isolate both proteins that are modified by the reactive group as well as interacting proteins. To illustrate this use, purified recombinant PAD4 was labeled with BFA and then incubated with MCF-7 WCE overnight to facilitate the formation of interactions between PAD4 and PAD4 binding proteins. PAD4 protein complexes were subsequently bound to streptavidin-agarose and subjected to multiple washes to remove nonspecifically bound proteins. PAD4 and any PAD4 binding proteins were then eluted from the resin, and Western blotting was used to detect for the presence of several known PAD4 binding proteins, including p53, HDAC1, and histone H3.^{8,33} The results of these experiments, which are depicted in Figure 7, demonstrate that this approach can be used to isolate all three proteins, thereby demonstrating the potential utility of these compounds in identifying novel PAD4 binding proteins. An additional benefit of using the probes for identifying and characterizing PAD4 binding proteins comes from the fact that there is no interference, or additional signals, due to the presence of the heavy and light IgG chains, as occurs in Western blots of co-immunoprecipitated proteins.

Identification of PAD4 by Mass Spectrometry. To obtain a complete understanding of the factors that regulate *in vivo* PAD4 activity, the numbers, types, and the specific residues that undergo post-translational modifications need to be identified. To demonstrate the utility of the ABPPs for this application, the biotinylated probes were used to isolate endogenous PAD4 from HL60 granulocytes. Note that HL60 granulocytes were used because endogenous PAD4 is highly expressed in these cells and this cell line grows in suspension, thereby easing the isolation of high amounts of biomass. Proteins were then separated by SDS-PAGE, and a band corresponding to the size of PAD4 was excised from the gel and subjected to in-gel tryptic digestion. The identities of isolated peptides were then determined by MALDI mass spectrometry. Overall sequence coverage of 60.6% was obtained (Figure 8 and Table S2). The identities of select peptide fragments were further validated by performing MS/MS sequencing (see Figure S5 for representative MS/MS spectra). The results of these experiments further confirm that these ABPPs can be used to isolate PAD4 and demonstrate their future use to identify novel post-translational modifications that occur to PAD4 under various physiological conditions.

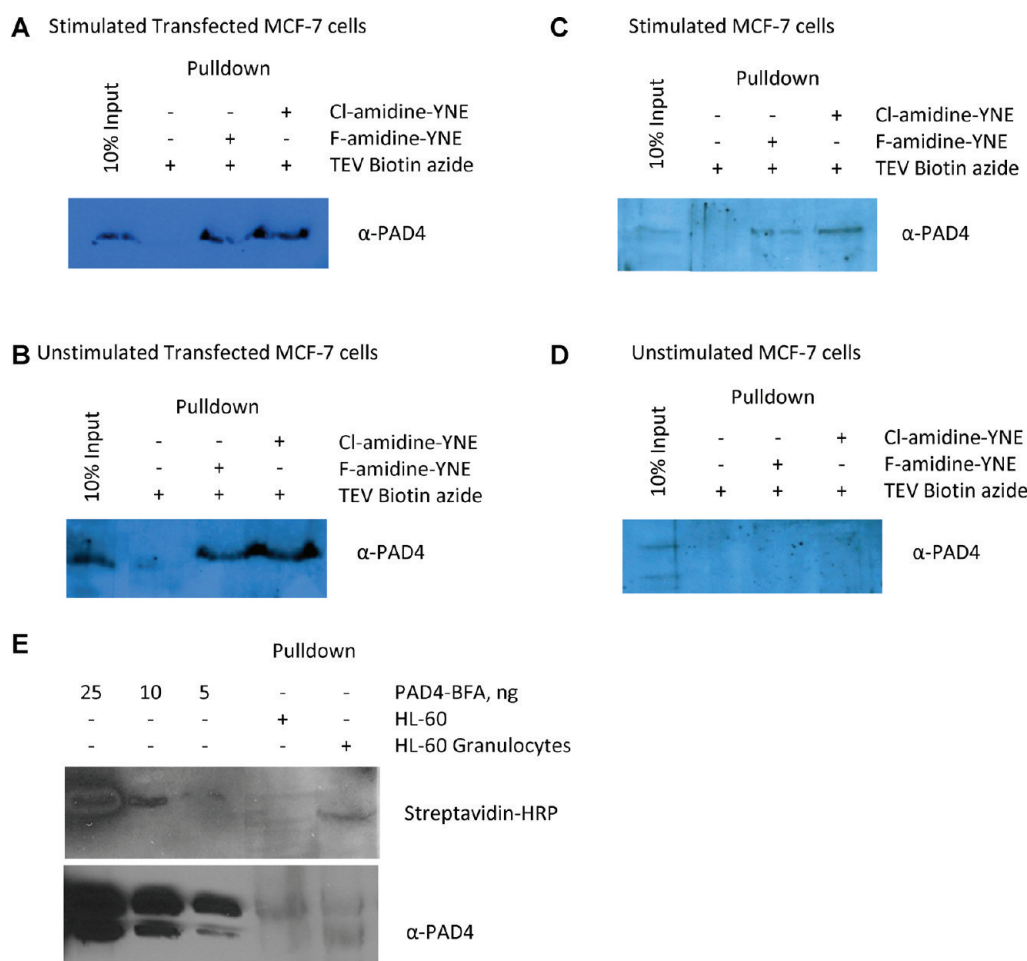


Figure 5. Post-inactivation coupling experiments using live MCF-7 cells. MCF-7 cells were treated with either F- or Cl-amidine-YNE for 60 min. The cells were lysed, and the extracts were subsequently coupled to TEV-biotin-azide. The probed modified proteins were enriched on streptavidin agarose and visualized by Western blot using an α -PAD4 antibody. (A) PAD4 transfected MCF-7 cells, stimulated with estrogen. (B) PAD4 transfected MCF-7 cells, unstimulated. (C) Untransfected MCF-7 cells, stimulated with estrogen. (D) Untransfected MCF-7 cells, unstimulated. (E) Selectivity of probes for activated endogenous PAD4. HL-60 cells and HL-60 granulocytes were treated with F-amidine-YNE for 45 min. The cells were lysed, and the extracts were subsequently coupled to TEV-biotin-azide. The probe-modified proteins were visualized by Western blot using either streptavidin-HRP (top) or an anti-PAD4 antibody.

In total, the ABPPs described herein provide a unique suite of tools that can be used to label PAD4 in cells, as well as for isolating PAD4 and PAD4 binding proteins. These probes will undoubtedly prove useful in identifying and characterizing the post-translational modifications and binding proteins that regulate PAD4 activity as well as dissecting the factors controlling the dynamics of PAD4 expression.

METHODS

Synthesis of ABPPs. Refer to Supporting Information and methods.

IC₅₀ Values. IC₅₀ values were determined, in either the absence or presence of calcium, using methods established in the Thompson lab.²² The data were fit to eq eq 1

$$\text{fractional activity of PAD} = 1/(1 + [I]/IC_{50}) \quad (\text{eq 1})$$

, using Grafit 5.0.1.1.³⁴ All measurements were made at least in duplicate and the values obtained generally agreed within 20%.

In Vitro Labeling of Wild Type PAD4 with FXA Probes. To determine the optimal probe concentration for labeling PAD4 with

FFA1 and FCA1, purified recombinant wild type PAD4 (2.5 μ g) was incubated at 37 °C in reaction buffer (50 mM HEPES pH 7.6, 2 mM DTT, 50 mM NaCl) containing various concentrations (2, 5, 10, and 20 μ M) of either FFA1 or FCA1, in either the absence or presence of calcium (10 mM final) for 1 h. To determine the limits of detection for both FFA1 and FCA1, purified recombinant wild type PAD4 (0.125–2.5 μ g) was incubated at 37 °C in reaction buffer containing either 20 μ M FFA1 or FCA1 for 1 h. Standard 6X SDS-PAGE loading buffer (4 μ L) was added to each sample (20 μ L) to quench the reaction. Subsequently the samples were boiled for 30 min, and then the proteins were separated on a 12% SDS-PAGE gel. Labeled proteins were visualized in-gel using a molecular imaging station (Kodak Image Station 2000MM) using an excitation filter of 465 nm and an emission filter of 535 nm.

In Vitro Labeling of Wild Type PAD4 with BFA and BCA. To determine optimal probe concentration for labeling PAD4 with BFA and BCA, purified recombinant wild type PAD4 (2.5 μ g) was incubated at 37 °C in reaction buffer containing various concentrations (2, 5, 10, and 20 μ M) of BFA or BCA in either the presence or absence of calcium (10 mM final) for 1 h. To determine the limits of detection for BFA and BCA, purified recombinant wild type PAD4 (0.05 to 2.5 μ g) was incubated at 37 °C in reaction buffer containing either 5 μ M of BFA or BCA for 1 h. Samples were processed for SDS-PAGE as described above.

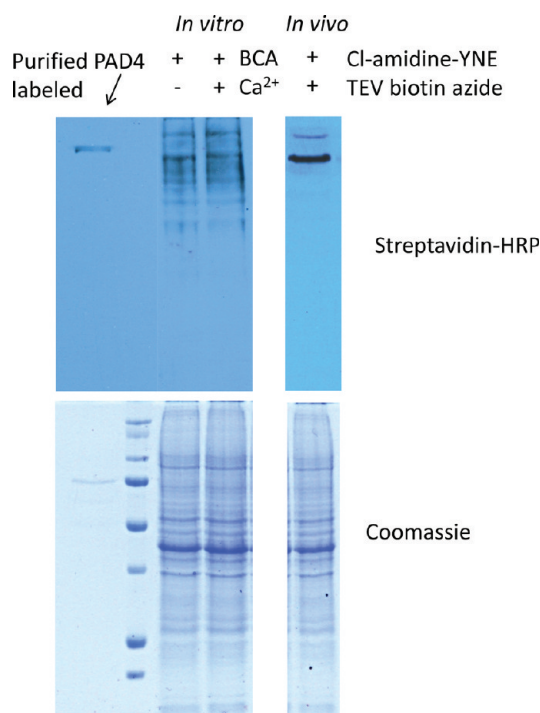


Figure 6. Comparison of labeling methods. (A) Labeling of MCF-7 whole cell extracts with BCA. Extracts, prepared from estrogen-stimulated MCF7 cells, were incubated with BCA (1 μ M) for 30 min at 37 °C. The labeled proteins were visualized by Western blotting using streptavidin-conjugated HRP. (B) Post-inactivation coupling in live MCF-7 cells. Live estrogen-stimulated MCF-7 cells were treated with Cl-amidine-YNE (100 μ M) for 60 min. Cells were lysed in RIPA buffer (25 mM Tris HCl pH 7.6, 150 mM NaCl, 1% NP-40, 1% sodium deoxycholate, 0.1% SDS) on ice for 10 min. The samples were denatured at 95 °C for 10 min prior to the addition of the TEV-biotin-azide reporter tag (20 μ M). The click reaction was then initiated by the addition of TCEP (2.5 mM), ligand (0.119 mM final), and CuSO₄ (5 mM final). The labeled proteins were visualized by Western blotting using streptavidin-conjugated HRP.

Proteins were then transferred to a nitrocellulose membrane at 80 V for 70 min in CAPS transfer buffer (9 mM CAPS, 10% methanol pH 11). The membranes were blocked with 5% BSA in PBS overnight, washed with PBS twice for 10 min, and incubated with streptavidin-conjugated HRP (Invitrogen; 1:10,000) in 2.5% BSA in PBS. Membranes were rinsed twice with PBS for 10 min, and HRP signals were detected using the Pierce ECL Western blotting substrate (catalogue no. 32106, Thermo Scientific). Image J was used to quantify the intensity of labeling, and the detection limits were defined as a 2.5-fold signal over background.

In Vitro Labeling of Endogenous PAD4 in MCF-7 WCE. To determine optimal probe concentration for labeling endogenous PAD4 with BFA, MCF-7 whole cell extracts (WCE) were precleared on streptavidin agarose for 30 min at 4 °C. Various concentrations of BFA (2, 5, 10, and 20 μ M) were added to the precleared WCE and incubated at 37 °C in reaction buffer (50 mM Tris-HCl pH 7.6, 50 mM NaCl, 2 mM DTT, 10 mM CaCl₂) for 30 min. Samples were processed for SDS-PAGE as described above. Proteins were then transferred to a nitrocellulose membrane at 80 V for 70 min in CAPS transfer buffer (9 mM CAPS, 10% methanol pH 11). The membranes were probed with streptavidin-conjugated HRP to detect the probe-modified proteins.

Enrichment of Probe-Modified Proteins with BFA and BCA. Purified recombinant wild type PAD4 (2.5 μ g) and *E. coli* extracts overexpressing GST-PAD4 (5 μ g total protein) were incubated in reaction buffer containing 10 μ M of either BFA or BCA, in the presence of

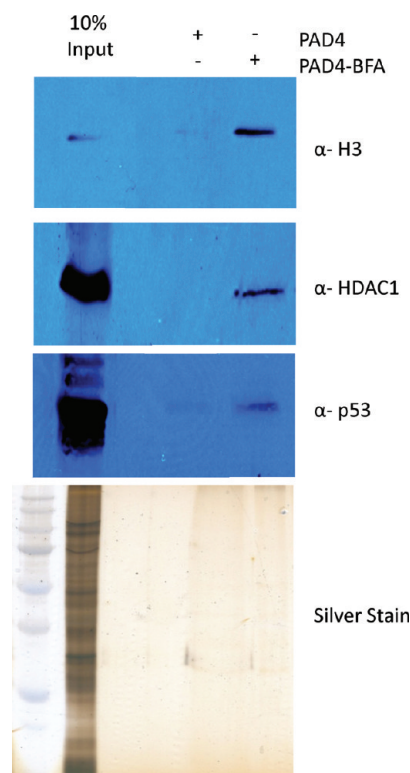


Figure 7. Enrichment of known PAD4 binding partners using BFA-labeled PAD4. PAD4 and PAD4 labeled with BFA were incubated with MCF-7 whole cell extracts. PAD4 complexes were enriched on streptavidin agarose beads and probed with antibodies for (A) Histone H3, (B) HDAC1, and (C) p53.

CaCl₂ (10 mM final) at 37 °C. After 30 min, 1.2% SDS in PBS was added to each reaction, and the proteins were denatured at 95 °C for 5 min. The denatured proteins were then added to 100 μ L of streptavidin-agarose beads in PBS and incubated overnight at 4 °C. The beads were washed by adding 500 μ L of 0.2% SDS/PBS for 10 min and collected by centrifugation (1,400g, 3 min). The supernatant was removed, and the beads were washed with PBS (3 \times 5 mL). To elute the bound proteins, streptavidin-agarose beads were incubated in buffer A (1% SDS, 15 mM biotin, 100 mM thiourea, 3 M urea in PBS) for 1 h at 42 °C followed by 30 min at 95 °C. The supernatant was then removed, and the beads were washed with water three times. The supernatant and wash fractions were combined and concentrated to approximately 20 μ L. The entire sample was loaded onto a 12% SDS-PAGE, and proteins were visualized by coomassie blue staining.

Post-inactivation Coupling. Purified recombinant wild type PAD4 (2.5 μ g) was treated with either 20 μ M X-amidine-YNE or X-amidine-azide in the presence of 1 mM CaCl₂, 50 mM HEPES pH 7.6, 2 mM DTT and 50 mM NaCl for 30 min at 37 °C. The alkyne- or azide-modified proteins were then labeled, *via* the copper(I)-catalyzed azide-alkyne [3 + 2] cycloaddition reaction, with either the TEV-biotin-azide reporter tag or the FITC-reporter tags containing the complementary alkyne/azide. The click reaction was performed using a slight modification of previously established procedures.²⁵ Briefly, modified proteins were reacted with the corresponding azide or alkyne reporter tag (20 μ M final) in the presence of TCEP (2.5 mM), ligand (0.119 mM final), and CuSO₄ (5 mM final).²⁵ After incubating at rt for 1 h, as described,²⁵ the samples were centrifuged (5000 rpm, 4 °C) and the protein pellet was washed with cold methanol (2 \times 100 μ L). The pellet was resuspended in 15 μ L SDS buffer (2% SDS, 62.5 mM Tris pH 6.8, 10% glycerol in PBS) and separated on 12% SDS-PAGE gels. Fluorescently tagged proteins were

PAD4 Digest- 60.6% sequence coverage

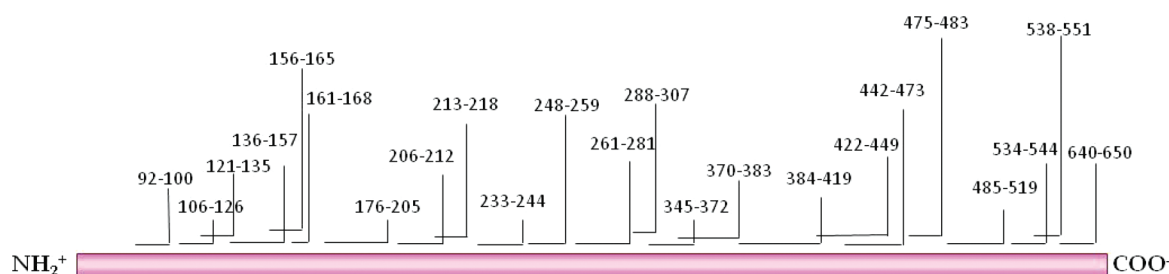


Figure 8. PAD4 peptide mass fingerprint obtained from in-gel digests performed on endogenous PAD4 isolated from mammalian cells. Sequence coverage is 60.6%.

visualized using a Kodak Image Station 2000MM molecular imaging system. Biotinylated proteins were visualized by Western blot using streptavidin-conjugated HRP after transfer to a nitrocellulose membrane.

Transfection. MCF-7 cells were grown to a confluence of ~90% in DMEM media containing 10% FBS at 37 °C and 5% CO₂. Cells were transiently transfected with human PAD4 using the Lipofectamine 2000 reagent from Invitrogen (cat. 11668).⁸ A DNA to Lipofectamine ratio of 1:2.5 was used. After transfection, the cells were incubated at 37 °C and 5% CO₂ for 24 h to allow for recovery prior to the post-inactivation coupling experiments.

In Vivo Post-inactivation Coupling. Transfected and non-transfected MCF-7 cells were incubated with either X-amidine-YNE (100 μM final) in either the absence or presence of estrogen (0.1 μM final) for 1 h at 37 °C and 5% CO₂. Subsequently the cells were harvested and lysed in RIPA buffer (25 mM Tris HCl pH 7.6, 150 mM NaCl, 1% NP-40, 1% sodium deoxycholate, 0.1% SDS) on ice for 10 min. The samples were denatured at 95 °C for 10 min prior to the addition of either FITC-azide (20 μM) or the TEV-biotin-azide reporter tag. The click reaction was then initiated by the addition of TCEP (2.5 mM), ligand (0.119 mM final), and CuSO₄ (5 mM final). After 1 h at RT, the protein samples were collected by centrifugation (5000 rpm, 4 °C) and processed using the methodology described above.

Selectivity of ABPPs for Activated PAD4. HL-60 cells and HL-60 granulocytes, resuspended in Locke solution (5 mL), were incubated with F-amidine-YNE (100 μM final) in the presence of LPS (100 ng/mL) for 45 min. The cells were subsequently collected and lysed in RIPA buffer (25 mM Tris HCl pH 7.6, 150 mM NaCl, 1% sodium deoxycholate, 0.1% SDS). The samples were denatured at 95 °C for 10 min prior to the addition of the TEV-biotin-azide reporter tag (20 μM). Coupling of the reporter tag was initiated by the addition of TCEP (2.5 mM), ligand (0.119 mM final), and CuSO₄ (5 mM final). After incubating at rt for 1 h, the samples were centrifuged (5000 rpm, 4 °C), and the protein pellet was washed with cold methanol (2 × 100 μL). The pellet was resuspended in 15 μL of SDS buffer (2% SDS, 62.5 mM Tris pH 6.8, 10% glycerol in PBS) and separated on 12% SDS-PAGE gels. Proteins were transferred to a nitrocellulose membrane as described above and either probed with streptavidin-conjugated HRP or anti-PAD4.

Identification of PAD4-Binding Proteins. PAD4 (5 μg) was labeled with 1 μM BFA for 30 min at 37 °C in reaction buffer (50 mM Tris-HCl pH 7.6, 50 mM NaCl, 2 mM DTT, 10 mM CaCl₂). Labeled PAD4 (5 μg) was then added to MCF-7 whole cell extracts (500 μg total protein) and streptavidin-agarose beads (100 μL). After an overnight incubation at 4 °C with end over end rocking, the beads were washed three times with PBS. The beads were then washed with PBS + 100 mM NaCl and PBS + 250 mM NaCl. The higher salt wash was concentrated down to approximately 30 μL and separated on a 12% SDS-PAGE gel. Gels were transferred to a nitrocellulose membrane and probed with either a mouse monoclonal anti-p53 (abcam, ab1101) or a rabbit polyclonal anti-H3 (abcam, ab1791).

Identification of PAD4 by Mass Spectrometry. HL-60 granulocytes were incubated with F-amidine-YNE (100 μM final) in the presence of a calcium ionophore, A23817 (4 μM) for 1 h at 37 °C and 5% CO₂. Subsequently the cells were harvested and lysed in modified RIPA buffer (25 mM Tris HCl pH 7.6, 150 mM NaCl, 1% NP-40, 1% sodium deoxycholate) containing a complete protease inhibitor tablet (Roche) on ice. The click reaction was performed as described above. The entire sample was loaded onto a 12% SDS-PAGE, and proteins were visualized by Coomassie Blue staining. A protein band corresponding to the molecular weight of PAD4 was excised from the gel and subjected to an in-gel tryptic digestion. In-gel digestion was performed as previously described using the following proteases: trypsin, Glu-C, and Asp-N.³⁵ Peptides were concentrated in a speedvac to a final volume of ~30 μL, desalted using a C18 ZipTip (Millipore), and eluted in 2.5 μL of α-cyano hydroxycinnamic acid for analysis on an Ultraflex MALDI-TOF/TOF (Bruker Daltonics, Germany). Predicted peptide masses produced from the individual protease digestions were generated with ProteinProspector using the unmodified amino acid sequence of PAD4. Several individual peptides corresponding to the generated predicted masses were further confirmed to be PAD4 peptides by MS/MS fragmentation.

■ ASSOCIATED CONTENT

S Supporting Information. Synthetic procedures, supplemental experimental methods, Scheme S1, Figures S1–S5, Table S1. This information is available free of charge *via* the Internet at <http://pubs.acs.org>.

■ AUTHOR INFORMATION

Corresponding Author

*pthompso@scripps.edu

■ ACKNOWLEDGMENT

This work was supported by funds provided from National Institutes of Health grant GM079357.

■ REFERENCES

- (1) Jones, J. E., Causey, C. P., Knuckley, B., Slack-Noyes, J. L., and Thompson, P. R. (2009) Protein arginine deiminase 4 (PAD4): Current understanding and future therapeutic potential. *Curr. Opin. Drug Discovery Dev.* 12, 616–627.
- (2) Thompson, P. R., and Fast, W. (2006) Histone citrullination by protein arginine deiminase: Is arginine methylation a green light or a roadblock?. *ACS Chem. Biol.* 1, 433–441.
- (3) Vossenaar, E. R., and Van Venrooij, W. J. (2004) Citrullinated proteins: sparks that may ignite the fire in rheumatoid arthritis. *Arthritis Res. Ther.* 6, 107–111.

- (4) Vossenaer, E. R., Zendman, A. J., van Venrooij, W. J., and Pruijn, G. J. (2003) PAD, a growing family of citrullinating enzymes: genes, features and involvement in disease. *Bioessays* 25, 1106–1118.
- (5) Nakashima, K., Hagiwara, T., and Yamada, M. (2002) Nuclear localization of peptidylarginine deiminase V and histone deimination in granulocytes. *J. Biol. Chem.* 277, 49562–49568.
- (6) Hagiwara, T., Nakashima, K., Hirano, H., Senshu, T., and Yamada, M. (2002) Deimination of arginine residues in nucleophosmin/B23 and histones in HL-60 granulocytes. *Biochem. Biophys. Res. Commun.* 290, 979–983.
- (7) Nakashima, K., Hagiwara, T., Ishigami, A., Nagata, S., Asaga, H., Kuramoto, M., Senshu, T., and Yamada, M. (1999) Molecular characterization of peptidylarginine deiminase in HL-60 cells induced by retinoic acid and 1 α ,25-dihydroxyvitamin D(3). *J. Biol. Chem.* 274, 27786–27792.
- (8) Li, P., Yao, H., Zhang, Z., Li, M., Luo, Y., Thompson, P. R., Gilmour, D. S., and Wang, Y. (2008) Regulation of p53 target gene expression by peptidylarginine deiminase 4. *Mol. Cell. Biol.* 28, 4745–4758.
- (9) Cuthbert, G. L., Daujat, S., Snowden, A. W., Erdjument-Bromage, H., Hagiwara, T., Yamada, M., Schneider, R., Gregory, P. D., Tempst, P., Bannister, A. J., and Kouzarides, T. (2004) Histone deimination antagonizes arginine methylation. *Cell* 118, 545–553.
- (10) Wang, Y., Wysocka, J., Sayegh, J., Lee, Y. H., Perlin, J. R., Leonelli, L., Sonbuchner, L. S., McDonald, C. H., Cook, R. G., Dou, Y., Roeder, R. G., Clarke, S., Stallcup, M. R., Allis, C. D., and Coonrod, S. A. (2004) Human PAD4 regulates histone arginine methylation levels via demethylimination. *Science* 306, 279–283.
- (11) Hagiwara, T., Hidaka, Y., and Yamada, M. (2005) Deimination of histone H2A and H4 at arginine 3 in HL-60 granulocytes. *Biochemistry* 44, 5827–5834.
- (12) Arita, K., Hashimoto, H., Shimizu, T., Nakashima, K., Yamada, M., and Sato, M. (2004) Structural basis for Ca²⁺-induced activation of human PAD4. *Nat. Struct. Mol. Biol.* 11, 777–783.
- (13) Kearney, P. L., Bhatia, M., Jones, N. G., Luo, Y., Glascock, M. C., Catchings, K. L., Yamada, M., and Thompson, P. R. (2005) Kinetic characterization of protein arginine deiminase 4: A transcriptional corepressor implicated in the onset and progression of rheumatoid arthritis. *Biochemistry* 44, 10570–10582.
- (14) Knuckley, B., Bhatia, M., and Thompson, P. R. (2007) Protein arginine deiminase 4: Evidence for a reverse protonation mechanism. *Biochemistry* 46, 6578–6587.
- (15) Mechin, M. C., Enji, M., Nachat, R., Chavanas, S., Charveron, M., Ishida-Yamamoto, A., Serre, G., Takahara, H., and Simon, M. (2005) The peptidylarginine deiminases expressed in human epidermis differ in their substrate specificities and subcellular locations. *Cell. Mol. Life Sci.* 62, 1984–1995.
- (16) Nakayama-Hamada, M., Suzuki, A., Kubota, K., Takazawa, T., Ohsaka, M., Kawaida, R., Ono, M., Kasuya, A., Furukawa, H., Yamada, R., and Yamamoto, K. (2005) Comparison of enzymatic properties between hPAD12 and hPAD14. *Biochem. Biophys. Res. Commun.* 327, 192–200.
- (17) Musse, A. A., Polverini, E., Raijmakers, R., and Harauz, G. (2008) Kinetics of human peptidylarginine deiminase 2 (hPAD2)—reduction of Ca²⁺ dependence by phospholipids and assessment of proposed inhibition by paclitaxel side chains. *Biochem. Cell Biol.* 86, 437–447.
- (18) Speers, A. E., and Cravatt, B. F. (2004) Profiling enzyme activities in vivo using click chemistry methods. *Chem. Biol.* 11, 535–546.
- (19) Jessani, N., and Cravatt, B. F. (2004) The development and application of methods for activity-based protein profiling. *Curr. Opin. Chem. Biol.* 8, 54–59.
- (20) Speers, A. E., and Cravatt, B. F. (2004) Chemical strategies for activity-based proteomics. *ChemBioChem* 5, 41–47.
- (21) Luo, Y., Knuckley, B., Lee, Y. H., Stallcup, M. R., and Thompson, P. R. (2006) A fluoro-acetamidine based inactivator of protein arginine deiminase 4 (PAD4): Design, synthesis, and in vitro and in vivo evaluation. *J. Am. Chem. Soc.* 128, 1092–1093.
- (22) Luo, Y., Arita, K., Bhatia, M., Knuckley, B., Lee, Y. H., Stallcup, M. R., and Thompson, P. R. (2006) Inhibitors and inactivators of protein arginine deiminase 4: Functional and structural characterization. *Biochemistry* 45, 11727–11736.
- (23) Stone, E. M., Schaller, T. H., Bianchi, H., Person, M. D., and Fast, W. (2005) Inactivation of two diverse enzymes in the amidinotransferase superfamily by 2-chloroacetamidine: Dimethylargininase and peptidylarginine deiminase. *Biochemistry* 44, 13744–13752.
- (24) Knuckley, B., Causey, C. P., Pellechia, P. J., Cook, P. F., and Thompson, P. R. (2010) Haloacetamidine-based inactivators of protein arginine deiminase 4 (PAD4): evidence that general acid catalysis promotes efficient inactivation. *ChemBioChem* 11, 161–165.
- (25) Weerapana, E., Speers, A. E., and Cravatt, B. F. (2007) Tandem orthogonal proteolysis-activity-based protein profiling (TOP-ABPP)—a general method for mapping sites of probe modification in proteomes. *Nat. Protoc.* 2, 1414–1425.
- (26) Wang, Y., Hu, S., and Fast, W. (2009) A click chemistry mediated in vivo activity probe for dimethylarginine dimethylaminohydrolase. *J. Am. Chem. Soc.* 131, 15096–15097.
- (27) Speers, A. E., Adam, G. C., and Cravatt, B. F. (2003) Activity-based protein profiling in vivo using a copper(i)-catalyzed azide-alkyne [3 + 2] cycloaddition. *J. Am. Chem. Soc.* 125, 4686–4687.
- (28) Rostovtsev, V. V., Green, L. G., Fokin, V. V., and Sharpless, K. B. (2002) A stepwise Huisgen cycloaddition process: copper(I)-catalyzed regioselective “ligation” of azides and terminal alkynes. *Angew. Chem., Int. Ed.* 41, 2596–2599.
- (29) Tornøe, C. W., Christensen, C., and Meldal, M. (2002) Peptidotriazoles on solid phase: [1,2,3]-triazoles by regioselective copper(i)-catalyzed 1,3-dipolar cycloadditions of terminal alkynes to azides. *J. Org. Chem.* 67, 3057–3064.
- (30) Luo, Y., Knuckley, B., Bhatia, M., and Thompson, P. R. (2006) Activity based protein profiling reagents for protein arginine deiminase 4 (PAD4): Synthesis and in vitro evaluation of a fluorescently-labeled probe. *J. Am. Chem. Soc.* 128, 14468–14469.
- (31) Speers, A. E., and Cravatt, B. F. (2005) A tandem orthogonal proteolysis strategy for high-content chemical proteomics. *J. Am. Chem. Soc.* 127, 10018–10019.
- (32) Slack, J. L., Causey, C. P., and Thompson, P. R. (2010) Protein arginine deiminase 4: a target for an epigenetic cancer therapy. *Cell. Mol. Life Sci.* 68, 709–720.
- (33) Denis, H., Deplus, R., Putmans, P., Yamada, M., Metivier, R., and Fuks, F. (2009) Functional connection between deimination and deacetylation of histones. *Mol. Cell. Biol.* 29, 4982–4993.
- (34) Leatherbarrow, R. J. (2007) *GraFit Version 6*, 6.0 ed., Erithacus Software Limited, Horley, U.K.
- (35) Shevchenko, A., Tomas, H., Havlis, J., Olsen, J. V., and Mann, M. (2006) In-gel digestion for mass spectrometric characterization of proteins and proteomes. *Nat. Protoc.* 1, 2856–2860.